



ELSEVIER

Nuclear Instruments and Methods in Physics Research B 182 (2001) 56–61

NIM B
Beam Interactions
with Materials & Atoms

www.elsevier.com/locate/nimb

Thin-film effects on the surface stopping power of a free electron gas

A. Garcia-Lekue ^{a,*}, J.M. Pitarke ^{a,b}^a *Materia Kondentsatuaren Fisika Saila, Zientzi Fakultatea, Euskal Herriko Unibertsitatea, 644 Posta kutxatila, 48080 Bilbo, Basque Country, Spain*^b *Donostia International Physics Center (DIPC) and Centro Mixto CSIC-UPV/EHU, Donostia, Basque Country, Spain*

Abstract

The electronic properties of thin films present quantum-size effects (QSE), which are a consequence of the finite size of the system. Here we focus on the investigation of QSE on the electronic energy loss of charged particles moving parallel with metallic thin films. The energy loss is calculated within linear response theory, from the knowledge of the density-response function of the inhomogeneous system, which we evaluate either in the random-phase approximation or with the use of an adiabatic and local exchange-correlation kernel. © 2001 Elsevier Science B.V. All rights reserved.

PACS: 71.45.Gm; 79.20.Nc; 34.50.Bw

Keywords: Electronic energy loss; Quantum size effects

1. Introduction

The interaction of moving ions with solids has represented an active field of basic and applied physics [1,2]. Charged particles moving near metallic surfaces lose energy as a consequence of the creation of different excitations on the metal, such as electron–hole pairs and bulk and surface plasmons [3,4]. The theoretical understanding of electronic excitations is relevant in surface physics, as these modes are invariably involved in surface spectroscopies employing electrons, atoms, photons or ions [5–9].

In this paper we calculate self-consistently the energy-loss spectra of charged particles moving parallel to thin films or slabs, which are systems finite in one direction and infinite in the other two perpendicular directions. The electronic structure of the slabs is described by the jellium model, where the ions are replaced by a positive neutralizing background. Within this model the influence of the finite size was examined by Schulte [10], and he found an oscillatory behaviour of various physical properties as a function of the thickness of the slab. These effects can be observed experimentally and decrease as the size of the slab increases [11]. More recently, quantum-size effects (QSE) on the surface energy and work function of stabilized jellium slabs have

* Corresponding author. Fax: +34-4-464-8500.

E-mail address: wmbgalea@lg.ehu.es (A. Garcia-Lekue).

been examined [12]. Here we study the QSE on the energy-loss spectra of charged probe particles moving parallel to jellium slabs. From thin slab calculations and by means of the formula given in [13,14], infinite width-limit results are extrapolated, which can be compared with the self-consistent calculations for semi-infinite media in [15].

Energy-loss spectra and stopping power of jellium slabs are calculated in the frame of linear response theory and with use of the local density approximation (LDA) of density-functional theory (DFT) [16,17]. The dynamical density-response function is evaluated from the knowledge of the non-interacting density-response function within the random phase approximation (RPA) [18], or the adiabatic local-density approximation (ALDA): in the RPA long-range correlations are treated self-consistently, whereas short-range correlations are included in the ALDA [15]. The QSE on aluminium slabs are investigated and the results obtained in both approximations are compared. We also test the extrapolation formula previously mentioned.

In Section 2 we briefly present general expressions for the energy loss of charged particles moving parallel to a surface along a definite trajectory. Results are presented in Section 3. Section 4 summarizes the main conclusions. Atomic units are used unless otherwise stated, i.e., $e^2 = \hbar = m_e = 1$.

2. Theory

We consider a recoilless charged particle moving with constant velocity \mathbf{v} along a definite trajectory at a fixed distance z from a jellium surface. The interaction of the external particle with the electronic system creates a rearrangement of the density on the slab, and within the linear response theory this electronic density induced on the system is linearly related to the external field [19,20]. The system we are dealing with is translationally invariant along the z -direction and the stopping power in the frame of linear response can be expressed as [15]

$$-\frac{dE}{dx} = -\frac{2}{v} Z_1^2 \int \frac{d\mathbf{q}_{\parallel}}{(2\pi)^2} \times \int_0^{\infty} d\omega \omega \operatorname{Im} W(z, z; \mathbf{q}_{\parallel}, \omega) \delta(\omega - \mathbf{q}_{\parallel} \cdot \mathbf{v}), \quad (1)$$

where \mathbf{q}_{\parallel} and ω are the momentum transfer in the plane of the surface and the energy transfer, respectively. $\operatorname{Im} W(z, z; \mathbf{q}_{\parallel}, \omega)$ represents the screened interaction

$$W(z, z'; \mathbf{q}_{\parallel}, \omega) = v(z, z'; \mathbf{q}_{\parallel}) + \int dz_1 \int dz_2 v(z, z_1; \mathbf{q}_{\parallel}) \times \chi(z_1, z_2; \mathbf{q}_{\parallel}, \omega) v(z_2, z'; \mathbf{q}_{\parallel}), \quad (2)$$

where $v(z, z'; \mathbf{q}_{\parallel})$ and $\chi(z, z'; \mathbf{q}_{\parallel}, \omega)$ are two-dimensional Fourier transforms of the bare Coulomb potential and the density-response function, respectively [19].

The stopping power of the system can be described by means of $P(\omega)$, the total probability of exchanging energy ω with the medium

$$-\frac{dE}{dx} = \frac{1}{v} \int_0^{\infty} d\omega \omega P(\omega), \quad (3)$$

where

$$P(\omega) = -\frac{Z_1^2}{\pi^2 v} \int_0^{\infty} dq_x \operatorname{Im} W(z, z; \mathbf{q}_{\parallel}, \omega), \quad (4)$$

with $q_{\parallel} = \sqrt{q_x^2 + (\omega/v)^2}$. q_x is the component of the momentum in the direction of movement for a particle moving along the x axis.

The key ingredient of our calculation is the density-response function of the electron system, and within time-dependent density-functional theory (TDDFT) it satisfies *exactly* the following integral equation [21]:

$$\chi(z, z'; \mathbf{q}_{\parallel}, \omega) = \chi^0(z, z'; \mathbf{q}_{\parallel}, \omega) + \int dz_1 \times \int dz_2 \chi^0(z, z'; \mathbf{q}_{\parallel}, \omega) \times [v(z_1, z_2; \mathbf{q}_{\parallel}) + f_{xc}(z_1, z_2; \mathbf{q}_{\parallel}, \omega)] \times \chi(z_2, z'; \mathbf{q}_{\parallel}, \omega), \quad (5)$$

where $\chi^0(z, z_1; \mathbf{q}_{\parallel}, \omega)$ is the density-response function of non-interacting Kohn–Sham electrons, and

can be written in terms of the one-electron wavefunctions and eigenvalues [22].

$f_{xc}(z, z'; q_{\parallel}, \omega)$ is the Fourier transform of the exchange-correlation (xc) kernel $f_{xc}[n](\mathbf{r}, t; \mathbf{r}', t')$, which is the functional derivative of the time-dependent xc potential

$$f_{xc}[n](\mathbf{r}, t; \mathbf{r}', t') = \frac{\delta v_{xc}[n](\mathbf{r}, t)}{\delta n(\mathbf{r}', t')}. \quad (6)$$

Exchange-correlation effects are usually introduced within the local-density approximation (LDA) of DFT [16,17], by replacing the xc potential at z by that of a uniform electron gas of density $n(z)$. The xc kernel entering Eq. (5) is then set either equal to zero [this is the random-phase approximation (RPA)] or equal to the static ($\omega = 0$) xc kernel

$$f_{xc}(z, z'; q_{\parallel}, \omega) = \frac{dv_{xc}[n(z_1)]}{dn(z_1)} \delta(z_1 - z_2). \quad (7)$$

This is the so-called ALDA.

We consider jellium slabs of thickness a normal to the z -axis, consisting of a fixed uniform positive background of density

$$n_+(z) = \begin{cases} \bar{n}, & -a \leq z \leq a, \\ 0 & \text{elsewhere,} \end{cases} \quad (8)$$

plus a neutralizing cloud of interacting electrons of density $n(z) \cdot \bar{n} = q_F^3/3\pi^2$, where $q_F = (9\pi/4)^{1/3}/(r_s a_{\pm})$ is the Fermi wave vector, r_s is the Wigner-Seitz radius and a_0 is the Bohr radius.

QSE are originated by the quantization of the energy levels normal to the surface: as the slab-thickness a increases new sub-bands become occupied, thereby leading to oscillatory functions of a (the amplitude of these oscillations decays approximately linearly with a , and their period equals $\lambda_F/2$, $\lambda_F = 2\pi/q_F$ being the Fermi wavelength). For each quantity α under study, we consider three different values of a . One such value is the threshold width a_n for which the n th sub-band for the z motion is first occupied. The other two are $a_n - \lambda_F/4$ and $a_n + \lambda_F/4$, and the infinite width limit is then extrapolated with the use of the following relation [13,14]:

$$\alpha = \frac{\alpha(a_n^-) + \alpha(a_n) + \alpha(a_n^+)}{3}. \quad (9)$$

These size effects are responsible for the oscillatory behaviour of the electronic density induced by the external probe on the surface, and consequently, for the oscillations of the energy loss and stopping power with the system size. The results presented below correspond to slabs with n between 11 and 14, for which $a \approx (4-7)\lambda_F$, depending on r_s .

To compute $\chi(z, z'; q_{\parallel}, \omega)$, we follow the method described in [23,24]. We first assume that $n(z)$ vanishes at a distance z_0 from the surface and expand the one-electron wave functions in a Fourier sine series. The distance z_0 and the number of sine functions kept in the expansion of the wave functions are chosen sufficiently large for our calculations to be insensitive to the precise values employed. We then introduce a double-cosine representation for the density-response function.

3. Results

We have investigated thin-film effects on the energy-loss spectra of Al slabs, for which $r_s = 2.07$ and $\lambda_F = 6.77$ a.u. The projectile charge is considered to be fixed to $Z_1 = +1$. The main ingredient in our calculations is the screened interaction $W(z, z'; q_{\parallel}, \omega)$. The imaginary part of the screened potential versus the thickness a of the slab in the RPA and ALDA for $q_{\parallel} = 0.4q_F$ and $\omega = 0.2\omega_p$, where ω_p is the classical bulk plasmon frequency, is shown in Fig. 1, which clearly exhibits the oscillatory character originated by the QSE. As a increases, new sub-bands for the z motion become occupied. Such a new sub-band falls below the Fermi level every time a is a multiple of $\lambda_F/2$. When a new sub-band is pulled below the Fermi level, the parallel Fermi sea built upon the newly occupied sub-band acquires more electrons, and the probability of exciting electron-hole pairs increases, as for these excitations transitions between states near the Fermi level are the most important. Consequently, the energy-loss probability of the system increases. However, this effect is eventually overcome by the fact that all the sub-bands for the

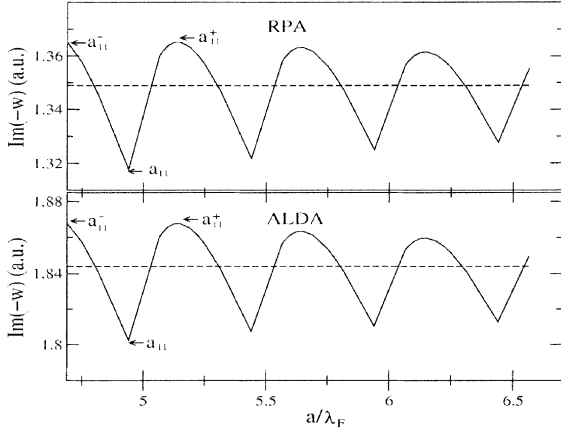


Fig. 1. Imaginary part of the screened interaction as a function of a in the RPA and ALDA, with $q_{\parallel} = 0.4q_F$, $\omega = 0.2\omega_p$ and $z = 2$ a.u. Dashed lines represent the infinite width limit, as given in Eq. (9). Damping parameter is equal to $\omega_p/10$.

z motion get deeper with increasing film thickness. When a has increased by $\lambda_F/2$, a new sub-band begins to be filled and a new oscillation begins. Both curves in Fig. 1 show damped oscillations with minima occurring at the slab width $a \sim n\lambda_F/2$. Dashed lines represent the results for the semi-infinite flat Al jellia obtained by means of Eq. (9). The relative amplitude of the oscillations is of $\sim 2\%$ for both approximations, although it is slightly larger in the RPA. This oscillatory behaviour is therefore present in all the physical magnitudes related to the screened interaction, such as energy loss and stopping power.

The influence of the short-range correlations on the energy loss is studied by employing the many-body kernel of Eq. (7). Introducing the xc kernel leads to a more effective screening of the electron–electron interaction in the ALDA compared with the RPA. As a result, the interaction of the external particle with the electronic system is larger. This is observed in Fig. 2, where the imaginary part of the screened potential is represented as a function of the distance from the external particle to the right edge of the slab in the RPA and ALDA for three different values of a corresponding to a local minimum and the two local maxima around it, as pointed in Fig. 1, with the same values of q_{\parallel} and ω as before. The infinite width limit is represented as well. We find that size effect

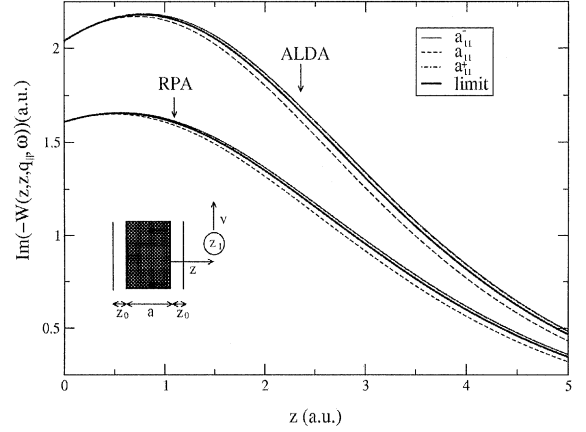


Fig. 2. Imaginary part of the screened interaction as a function of the distance to the jellium surface in the RPA and ALDA, for the three different values of the slab width pointed in Fig. 1 and for a semi-infinite slab. q_{\parallel} , ω and damping parameter as in Fig. 1.

become more significant as the particle moves away from the surface into the vacuum, which is due to the fact that as z increases the external field couples mainly with the plasmon modes. Since these are modes characterized by their long wavelength, their behaviour depends strongly on the overall size of the system. For particles moving close to the surface, the interaction has a short-range character, as the main contribution comes from the electron–hole pairs, i.e., modes with short wavelength. This leads to a decrease of the size effects, as the coupling involves electrons located near the surface, the dependence of these electrons upon the total width of the slab being not so relevant.

The same oscillatory behaviour is observed in Fig. 3 for the probability that an external particle that moves with velocity $v = 0.5$ a.u. at a distance $z = 2$ a.u. exchanges energy $\omega = 0.2\omega_p$ with an Al jellium slab.

In Fig. 4 we have represented the energy loss probability as a function of the transferred energy, when the external particle moves with velocity $v = 0.5$ a.u. at a distance $z = 2$ a.u. from the surface. Since exchange–correlation contribution weakens the bare Coulomb interaction the ALDA frequencies lie below those in the RPA. QSE are more evident for large energy transfers, i.e., for

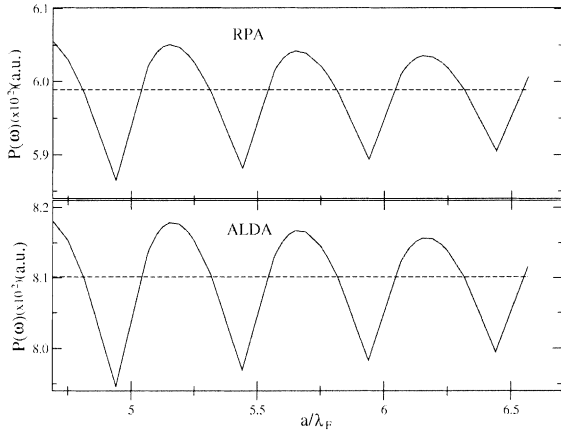


Fig. 3. Energy loss probability as a function of the slab size a with $z = 2$ a.u., $v = 0.5$ a.u. and $\omega = 0.2\omega_p$, in the RPA and ALDA. Dashed lines represent the infinite width limit. Damping parameter is equal to $\omega_p/10$.

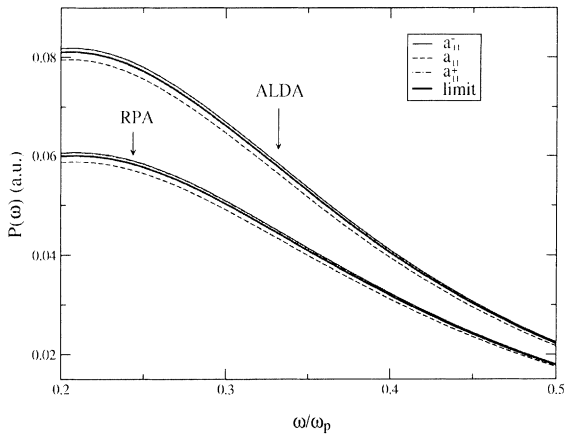


Fig. 4. Energy loss probability for a charged particle moving at a distance $z = 2$ a.u. from the surface of a semi-infinite slab with a velocity $v = 0.5$ a.u. in the RPA and ALDA as a function of the energy transfer ω for the same values of the slab width as in Fig. 2. Damping parameter is equal to $\omega_p/10$.

large values of ω , as in this case the energy loss is mainly due to the excitation of electron–hole pairs.

The dependence of the stopping power on the slab size, as obtained from Eq. (1) is exhibited in Fig. 5, both in the RPA and ALDA. We have considered an external probe particle moving with velocity $v = 2$ a.u. at a distance $z = 2$ a.u. from the right edge of the film. For these values of z and v

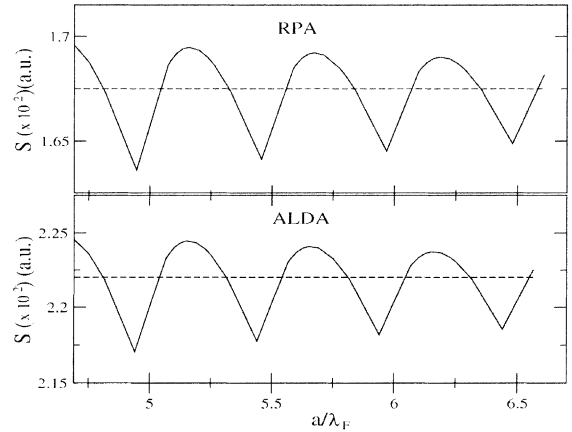


Fig. 5. Stopping power as a function of the slab size a for a particle moving with velocity $v = 0.5$ a.u. at a distance $z = 2$ a.u. from the right edge of the jellium slab, in the RPA and ALDA. Dashed lines represent the infinite width limit. Damping parameter is equal to $\omega_p/10$.

the ALDA results are significantly larger than those obtained using the RPA, which is a consequence of the larger electron–hole excitation probability present in the ALDA.

Fig. 6 shows the behaviour of the stopping power with the velocity for a projectile moving at a small distance from the surface into the vacuum,

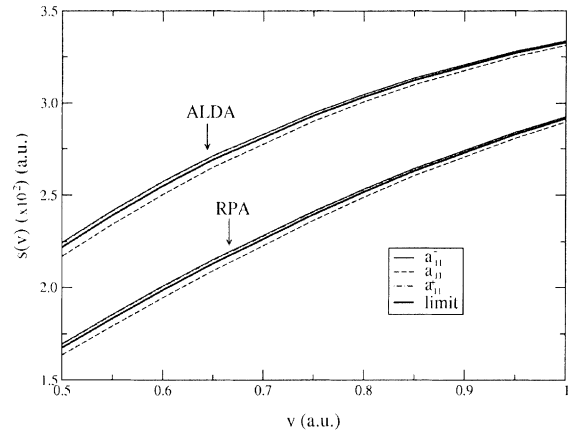


Fig. 6. Stopping power as a function of the velocity in the RPA and ALDA for an external particle moving at a distance $z = 2$ a.u. from the surface into the vacuum in the RPA and ALDA and for the three different values of the slab width pointed in Fig. 1 and for a semi-infinite slab. Damping parameter is equal to $\omega_p/10$.

$z = 2$ a.u. For very small values of v the electron–hole pairs are the dominant excitation modes, leading to a significant size effect. As the velocity increases plasmon modes start to play a role, and the QSE diminish. If we compare the ALDA and RPA results, we conclude that the impact of including exchange-correlation effects in the response is less important for larger values of the velocity. Larger velocities imply a larger contribution of small momentum components, and as for small values of q the Coulomb component dominates over the exchange-correlation component in Eq. (5), the ALDA results tend to those obtained by the RPA.

4. Conclusions

We have presented self-consistent calculations of the electronic energy loss of charged particles moving parallel to thin Al jelliums slabs. The ground state of the system has been calculated using LDA orbitals, whereas the RPA or ALDA approximations have been considered to compute the density-response function of the inhomogeneous system.

The oscillatory behaviour originated by the QSE is observed, which is a consequence of the finite size of the system. For both approaches, the screened interaction and consequently all the magnitudes related to it such as the energy loss probability and stopping power present oscillations as a function of the thickness of the slab. The period of these oscillations equals $\lambda_F/2$ and the amplitude, which is slightly higher in the RPA than in the ALDA, decays approximately linearly with a . The extrapolation formula given in [13,14] was employed to get the infinite width limit.

The screened interaction for given values of energy and momentum transfer present larger size effects as the external probe moves away from the surface into the vacuum, as a consequence of the stronger coupling of the external potential with plasmon modes. The dependence on the system

size of the energy loss probability of slowly moving particles is found to be relevant mainly for large energy transfer. We conclude that QSE on the stopping power of charged particles moving near the surface into the vacuum are more significant for smaller values of the velocity.

Acknowledgements

We acknowledge partial support by the Basque Unibertsitate eta Ikerketa Saila.

References

- [1] D.H. Schneider, M.A. Briere, *Phys. Scr.* 53 (1996) 228.
- [2] A. Arnau, et al., *Surf. Sci. Rep.* 27 (1997) 113.
- [3] D. Pines, *Solid State Phys.* 1 (1955) 367.
- [4] R.H. Ritchie, *Phys. Rev.* 106 (1957) 874.
- [5] H. Raether, in: G. Höhler (Ed.), *Springer Tracks in Modern Physics*, Vol. 88, Springer, Berlin, 1980.
- [6] P.E. Batson, *Phys. Rev. Lett.* 49 (1982) 936.
- [7] H. Kohl, *Ultramicroscopy* 11 (1983) 53.
- [8] R.H. Ritchie, A. Howie, *Philos. Mag.* A 58 (1988) 753.
- [9] D.W. McComb, A. Howie, *Nucl. Instr. and Meth.* B 96 (1995) 569.
- [10] F.K. Schulte, *Surf. Sci.* 55 (1976) 427.
- [11] R.C. Jaklevic, J. Lambe, *Phys. Rev. B* 12 (1975) 4146.
- [12] I. Sarria, C. Henriques, C. Fiolhais, J.M. Pitarke, *Phys. Rev. B* 62 (2000) 1699.
- [13] J.M. Pitarke, A.G. Eguiluz, *Phys. Rev. B* 57 (1998) 6329.
- [14] J.M. Pitarke, A.G. Eguiluz, *Phys. Rev. B* 63 (2001) 45116.
- [15] A. Garcia-Lekue, J.M. Pitarke, *Phys. Rev. B*, in press.
- [16] W. Kohn, L.J. Sham, *Phys. Rev.* 140 (1965) A11333.
- [17] P. Hohenberg, W. Kohn, *Phys. Rev.* 136 (1964) B864.
- [18] G.D. Mahan, *Many-Particle Physics*, Plenum, New York, 1981.
- [19] P. Nozieres, D. Pines, *The Theory of Quantum Liquids*, Benjamin, New York, 1966.
- [20] M. Echenique, F. Flores, R.H. Ritchie, in: E.H. Ehrenreich, D. Turbull (Eds.), *Solid State Physics*, Academic Press, New York, 1990.
- [21] E.K.U. Gross, J.F. Dobson, M. Petersilka, *Density functional theory II*, in: R.F. Nalajewski (Ed.), *Topics in Current Chemistry*, Vol. 181, Springer, Berlin, 1996.
- [22] A. Griffin, J. Harris, *Can. J. Phys.* 54 (1976) 1396.
- [23] A.G. Eguiluz, *Phys. Rev. Lett.* 51 (1983) 1907.
- [24] A.G. Eguiluz, *Phys. Rev. B* 31 (1985) 3303.